Numerical Simulations of Nonlinear Waves Generated by Submerged Bodies

Kang Kuk-Jin[*1]

잠수물체에 의하여 발생되는 비선형파의 수치 시뮬레이션

강 국 진

A fundamental study for the numerical scheme to simulate unsteady nonlinear waves by solving Euler equations is presented. First, a conservation form and a non-conservation form of the Euler equations with a free surface fitted coordinate system are compared. Next, a time splitting fractional step method and an alternating direction implicit(ADI) method for the time integration are compared. For the comparative study, flow calculations around a bottom bump in a channel and a NACA 0012 hydrofoil in a flume are performed. The results show that the ADI method with a third order upwind differencing scheme is very efficient in reducing the computing time with keeping the accuracy. And, there is no distinct difference between two expression forms except that the non-conservative form shows faster wave propagating velocity than the conservation form. Some results are compared with experiments and show good agreement.

Key Words : 비선형파(Nonlinear Wave), 오일러방정식(Euler Eq.), 유한체적법(FVM), 유한차분법(FDM), Bottom Bump, NACA 0012

1. Introduction

Flows with free surfaces remain as one of the most interesting problems in fluid mechanics and very important in the ship hydrodynamics. Up to now, many numerical schemes to solve the free surface problems by means of solving the Euler or Navier-Stokes equations have been developed. However, there are still more difficulties to be overcome for the treatment of free surface boundary condition, especially the turbulence condition. In the present paper, a fundamental study to simulate unsteady nonlinear waves is investigated for the development of an accurate and efficient numerical scheme to solve Euler equations. The governing equations are the two-dimensional Euler and continuity equations which are written in a conservation form and non-conservation form. Body-fitted coordinates and an Eulerian moving grid system are used to fit the body and the deforming free surface boundary. Velocity and pressure components of are evaluated at the staggered grid system. A time splitting fractional step method and an alternating direction implicit (ADI) method are used for the time

*1 정회원, 한국기계연구원 선박해양공학연구센터

integration. For the comparative study, flow calculations around a bottom bump in a channel and a NACA 0012 hydrofoil in a wind tunnel and a flume are performed at each. Computational results for the latter are compared to the experiments by Gregory[1] for the wind tunnel and Duncan[2] for the flume.

2. Numerical procedure

2.1 Governing equations

Two-dimensional Euler equations and the equation of continuity are expressed in a nondimensionalized form as follows;

(1) Continuity equation

$$\frac{\partial u_i}{\partial x_i} = 0 \tag{1}$$

(2) Momentum equations

○ Conservation form

$$\frac{\partial u_i}{\partial t} + \frac{\partial (u_i u_j)}{\partial x_j} = -\frac{\partial \phi}{\partial x_i} \tag{2}$$

○ Non-conservation form

$$\frac{\partial u_i}{\partial t} + u_j \frac{\partial u_i}{\partial x_j} = -\frac{\partial \phi}{\partial x_i} \tag{3}$$

The x direction is positive towards the right-hand side and y is positive upwards. The free stream velocity vector is parallel to the x axis and points in the same direction. All lengths and velocities are non-dimensionalized by a characteristic length L and the free stream velocity U_o, respectively.

The pressure ϕ is the static pressure p minus the hydrostatic component $-y F_n^{-2}$ and can be expressed as $\phi = p + \frac{y}{F_n^2}$, where $F_n = \frac{U_o}{\sqrt{gL}}$ is the Froude number and g is the gravity acceleration constant. The pressure variable ϕ is nondimensionalized by ρU_o^2.

The governing equations in Cartesian coordinate system are transformed into the body-fitted coordinates system, (ξ_i, τ), $t = \tau$ as follows:

(1) Continuity equation

$$\frac{1}{J} \frac{\partial}{\partial \xi^i} (A_k^i u_k) = 0 \tag{4}$$

(2) Momentum equations

○ Conservation form :

$$J \cdot \frac{\partial u_i}{\partial \tau} + \frac{\partial}{\partial \xi^j} \left\{ J \cdot u_i \frac{\partial \xi^j}{\partial t} + A_k^j u_i u_k \right\} = -\frac{\partial}{\partial \xi^j} (A_k^j \delta_i^k \phi) \tag{5}$$

○ Non-conservation form :

$$\frac{\partial u_i}{\partial \tau} + U_j \frac{\partial u_i}{\partial \xi^j} = -b_i^j \frac{\partial \phi}{\partial \xi^j} \tag{6}$$

where, $A_k^j = J \cdot b_k^j$, $a_j^k = \frac{\partial x^k}{\partial \xi^j}$

$$b_k^j = \frac{\partial \xi^j}{\partial x^k} = \frac{1}{J} (a_i \times a_l)^k$$

$$J = \partial_i \cdot (a_j \times a_k) = det(a^l{}_m)$$

$$U_j = \left(\frac{\partial \xi^j}{\partial t} + b_j^k u_k \right)$$

2.2 Computational schemes

(1) Time splitting fractional step scheme

The momentum equations can be expressed in explicit form for velocity and implicit form for pressure as follows:

○ Conservation form :

$$\frac{u_i^{n+1}-u_i^n}{\Delta t} = -\frac{1}{J}\frac{\Delta F_i^n}{\Delta \xi^j} - \frac{1}{J}\frac{\Delta Q_i^{n+1}}{\Delta \xi^j} \quad (7)$$

where, n = time step, Δt = time increment

$$F_i = Ju_i\left(\frac{\partial \xi^j}{\partial t} + b_j^k u_k\right) = Ju_i U_j \quad (8)$$

$$Q_i = (A_k^j \delta_i^k \phi) \quad (9)$$

○ Non-conservation form :

$$\frac{u_i^{n+1}-u_i^n}{\Delta t} = -U_j^n \frac{\partial u_i^n}{\partial \xi^j} - b_i^j \frac{\partial \phi^{n+1}}{\partial \xi^j} \quad (10)$$

The general vector form of the above equations can be written as follows:

$$\frac{q^{n+1}-q^n}{\Delta t} = -\nabla F^n - \nabla \phi^{n+1} \quad (11)$$

$$q^{n+1} = q^n + \Delta q^n - \Delta t \cdot \nabla(\delta \phi) \quad (12)$$

where, $q = \begin{pmatrix} u \\ v \end{pmatrix}$, $\phi^{n+1} = \phi^n + \delta\phi$ (13)

$$\Delta q^n = -\Delta t \cdot (\nabla F^n + \nabla \phi^n) \quad (14)$$

The solution procedure is as follows:

(a) Intermediate velocity calculation

$$\tilde{q} = q^n + \Delta q^n \quad (15)$$

(b) Velocity correction with $\delta\phi^m$

$$q^m = \tilde{q} - \Delta t \cdot \nabla(\delta \phi^m) \quad (16)$$

(c) Pressure correction with ∇q^m

$$\delta\phi^* = -\frac{\omega}{2g^{II}}\frac{\nabla q^m}{\Delta t} \quad (17)$$

$$\delta\phi^{m+1} = \delta\phi^m + \delta\phi^* \quad (18)$$

(b) and (c) are repeated until $|\delta\phi^*| < \varepsilon$. The maximum iteration number m is confined to 20 and $\varepsilon = 10^{-5}$ is used as the pressure convergence criterion for one time step.

(2) Alternating direction implicit(ADI) scheme

The implicit form of the momentum equations also can be written as eq. (12), but eq. (14) is replaced as follows:

$$\Delta q^n = -\Delta t \cdot (\nabla F^{n+1} + \nabla \phi^n) \quad (19)$$

Then, Δq^n is solved by the ADI method [3]. And the following procedures are as same the explicit scheme.

The pressure and the metric coefficients are approximated by the second-order central difference scheme. And the convective terms are discretized by the third-order upwind scheme. The grid system is generated by Steger's method[4]. A one-block and a two-block H-grid topology are used for the flow calculation around the bottom bump and the NACA 0012 hydrofoil at each. Grids move vertically in an Eulerian manner.

3. Boundary Conditions

3.1 Body boundary condition

The Euler solver requires the free-slip condition on the body boundary as follows:

$$\vec{u} \cdot \vec{n} = 0 \quad (20)$$

That is, the normal velocity component (V_1) should be zero and the tangential velocity component (U_1) is set to be equal to the most adjacent one (U_2) on the body. Here, U and

V are contravariant velocity vectors and calculated as follows:

$$U = u\xi_x + v\xi_y$$
$$V = u\eta_x + v\eta_y \quad (21)$$

From these relations, velocity components (u_1, v_1) on the body are calculated as follows:

$$u_1 = (u y_\eta - v x_\eta)_2 / (y_\eta - \frac{y_\xi}{x_\xi} x_\eta)_1 \quad (22)$$
$$v_1 = u_1 (\frac{y_\xi}{x_\xi})_1$$

3.2 Free surface boundary condition

The inviscid free surface conditions consist of the following two conditions. One is the dynamic condition which means that the pressure on the free surface is equal to the atmospheric pressure. For the inviscid case this is expressed as

$$\phi = p_o + \frac{h}{F_n^2} \qquad on \quad y = h \quad (23)$$

where p_o is atmospheric pressure (assumed to be 0 here) and $y = h(x; t)$ is the free surface location. The other is the kinematic condition which means the fluid particles on the free surface keep remaining on it, and written as follows;

$$\frac{\partial h}{\partial t} + u\frac{\partial h}{\partial x} - v = 0 \quad (24)$$

The free surface shape is updated by the following eq.

$$h^{n+1} = h^n + \Delta t \cdot (v - u h_\xi \xi_x)^{n+1} \quad (25)$$

From eq. (25), the following implicit equation is derived.

$$h^{n+1} + a \cdot u^{n+1} h_\xi^{n+1} = h^n + \Delta t \cdot v^{n+1} \quad (26)$$
$$\text{where,} \quad a = \Delta t \cdot \xi_x$$

Applying a 3rd-order upwind differencing scheme to eq. (26), the following penta-diagonal matrix is obtaind.

$$a \cdot h_{i-2} + b \cdot h_{i-1} + c \cdot h_i + d \cdot h_{i+1} + e \cdot h_{i+2} = q_i^n \quad (27)$$

where,

$$a = \frac{\alpha}{12}(u + |u|), \quad b = -\frac{\alpha}{3}(2u + |u|),$$
$$c = 1 + \frac{\alpha}{2}|u|, \quad d = \frac{\alpha}{3}(2u - |u|),$$
$$e = \frac{\alpha}{12}(|u| - u), \quad q_i^n = h^n + \Delta t \cdot v^{n+1}$$

The 2nd-order central differencing scheme is used for the ξ_x. Thus, the wave height of the (n+1)st time step is calculated by solving eq. (27). The velocity on the free surface is extrapolated from inside in such way that the velocity gradient in the normal direction is zero.

3.3 Other boundary conditions

Uniform flow and undisturbed free surface condition are imposed at the inflow boundary.

Zero-extrapolation method is used for the velocity and pressure at the outflow boundary. In addition, the following artificial wave damping method[5] is used to prevent the reflection of waves from the outflow boundary to the solution domain.

$$h^{n+1} = [h^n + \Delta t \cdot (v - u h_\xi \xi_x)^n] / [1 + \Delta t \cdot \gamma(x)] \quad (28)$$

where,

$$\gamma(x) = A(\frac{x - x_d}{x_o - x_d}), \quad \text{if } x_d \le x \le x_o \quad (29)$$

where A is a constant that controls the amount of damping (A=10 is used here) and

x_o is the x-coordinate of the outflow boundary. And x_d is defined as

$$x_d = x_o - 2\pi F_n^2 \quad (30)$$

4. Computational results

4.1 Bottom bump calculation

For the comparison of the three numerical schemes, numerical simulation of the waves generated by a bottom obstacle in a uniform flow was carried out. Hinatsu[6] showed the similar results about the same ploblem for the validation test of FDM scheme. The characteristic length L is taken as the water depth 1.0 while the height of bump is 0.5. The shape of bump is sinusoidal with a length of 4, and the length of the fluid domain is taken as 32. The free slip condition is used at the bottom boundary. The Froude number F_n is taken as 1.0 and the time increment $\triangle t$ is 0.01 for the FVM and the FDM, and $\triangle t$ is 0.1 for the ADI scheme. Figure 1 and 2 show the wave propagating patterns up to t=20. The results show good agreement with the Hinatsu's[6]. And there is no distinct difference among them even if ADI scheme take 10 times larger time increment than the others. However, ADI scheme needs much more iteration numbers to obtain divergence-free velocity field for one time step than the others.

4.2 NACA 0012 hydrofoil calculation

The characteristic length L is taken as the mid-chord length of the NACA 0012 hydrofoil.

(1) without free-surface

Flow calculation is performed at 6° incidence angle, which was tested in wind tunnel by Gregory[1]. The grid system ($i \times j = 114 \times 63$) with the minimum grid spacing $\triangle x_{min} = 0.001$, $\triangle y_{min} = 0.003$ is used for the calculation. The slip boundary condition is used at the top and bottom boundary, and $\triangle t = 0.0005$ for the FVM and the FDM, and $\triangle t = 0.005$ for the ADI scheme. Figure 3 shows that there is very small difference at the pressure peak zone. It shows good agreement with the experiments.

(2) with free-surface

Flow calculation is performed at 5^o incidence angle, which was tested in flume by Duncan[2]. The initial computational domain is taken as $-7.0 \leqq x \leqq 8.0$, $-1.8961 \leqq y \leqq 0.0$. The leading edge is located at $x/L = -0.25$. Pressure is assumed to zero and uniform flow condition is imposed on the bottom boundary. The minimum grid spacing $\triangle x_{min} = 0.001$, $\triangle y_{min} = 0.003$ and $\triangle t = 0.0005$ are used for the calculation.

For the grid dependency check, five cases of equal grid sizes($\triangle$x=0.02, 0.03, 0.05, 0.07, 0.1) are tested for three wave lengths after the trailing edge toward the positive ξ -direction. Calculations are carried out at F_n=0.567 and d/L=1.034, where d means the submerged depth.

Figure 4 shows the calculated velocity vectors and pressure contours around the foil at t=30. Figure 5, 6 show the convergence history of the pressure drag force coefficient C_{DF}, the lift force coefficient C_L and wave profile. From the Figure 6, it can be found that the solution was converged near t=25. Figure 7 shows the comparison of the calculated wave profiles together with the experimental data by Duncan. Fine grid systems show the more accurate wave profile, and the grid size $\triangle$x=0.03 is small enough for the accurate wave calculation. From these

results, it is found that the grid resolution has effect on the accuracy of the wave calculation and more than 50 grid points are necessary for one wave length to obtain the accurate wave profile. Hereafter, the grid size $\triangle x=0.03$ is used for all calculations. Figure 8 shows the comparison of the calculated wave profiles at various submerged depths. It is found that the breaking wave starts to occur near d/L=0.951 at F_n=0.567, where Duncan[2] showed that the transition from the steady non-breaking wave to the steady breaking wave exists there. Two kinds of wave breaking process are observed in the caculation, namely the first or second wave crest starts to break first. But there is no description on this phenomenon in the experiment.

5. Conclusions

A fundamental study for the numerical scheme to simulate unsteady nonlinear waves by solving Euler equations was performed and the following summary can be made.

(1) The ADI method with a third order upwind differencing scheme is efficient in reducing the computing time with keeping the accuracy.

(2) No distinct difference find out between two equation forms except that the FDM shows faster wave propagating velocity than FVM.

(3) The calculated results show good agreement with the experimental data.

(4) More than 50 grid points per one wave length are required to obtain the accurate wave profile for a submerged body.

(5) Further extensions of this method are the inclusion of viscous effects and generalization to three dimensions, etc.

Acknowledgment

This work was done while the author stayed at Chalmers University of Technology(CTH) as a visiting research fellow. He is grateful to the Korea Research Institute of Ships & Ocean Engineering, the Korea Science & Engineering Foundation and the Swedish Institute for the support during his stay at CTH. The author would like to thank Prof. Lars Larsson of CTH for having discussions about the computational results and offering facilities for the calculation.

References

[1] N. Gregory and C.L. O'Reilly, "Low-speed Aerodynamic Characteristics of NACA 0012 Aerofoil Section, including the Effects of Upper- Surface Roughness Simulating Hoar Frost", NPL Aero Report 1308, 1970

[2] Duncan J. H., "The breaking and non-breaking wave resistance of a two-dimensional hydrofoil", JFM, vol. 126, pp. 507~520, 1983.

[3] Y. Kodama, "Computation of High Reynolds Number Flows Past a Ship Hull using the IAF", Journal of the Society of Naval Architects of Japan, Vol. 161, 1987.

[4] Steger J. L. and Sorenson R. L., "Automatic Mesh-Point Clustering Near a Boundary in Grid Generation with Elliptic Partial Differential Equations", JCP, vol. 33, 1979.

[5] Hino T., "A Finite-Volume Method with Unstructured Grid for Free Surface Flow Simulations", 6th Int. Conf. on Numerical Ship Hydro, Iwoa, USA, 1993.

[6] Hinatsu M., "Numerical Simulation of Unsteady Viscous Waves Using Moving Grid System Fitted on a Free Surface", JKSNA, Japan, No. 217, March, 1992.

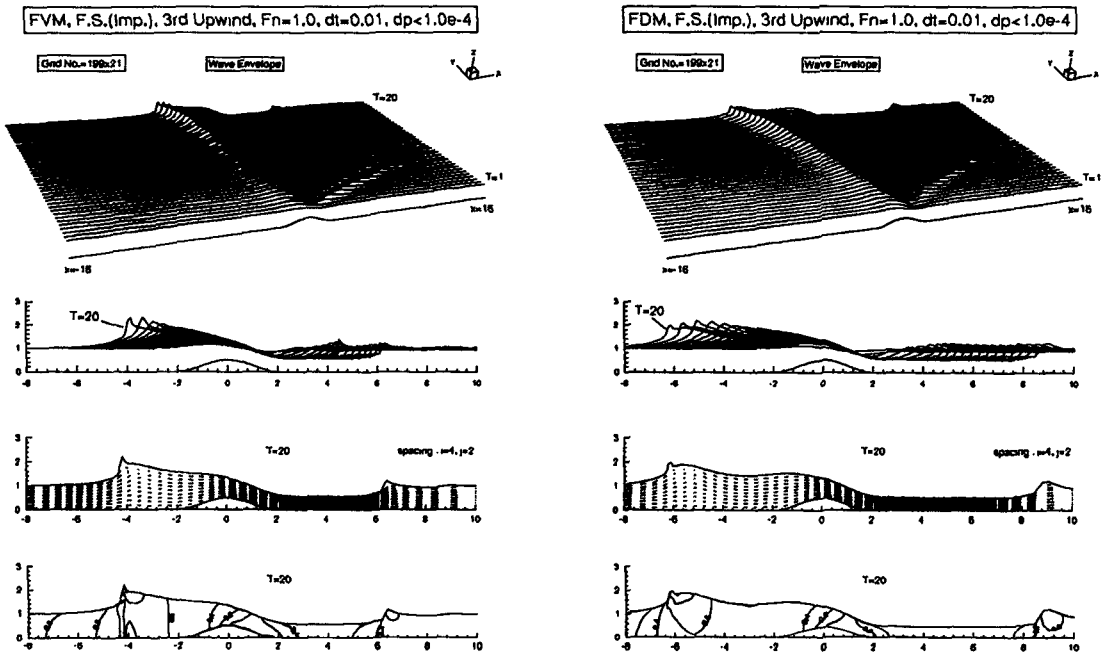

Fig. 1 Comparison of wave profile (FVM, FDM)

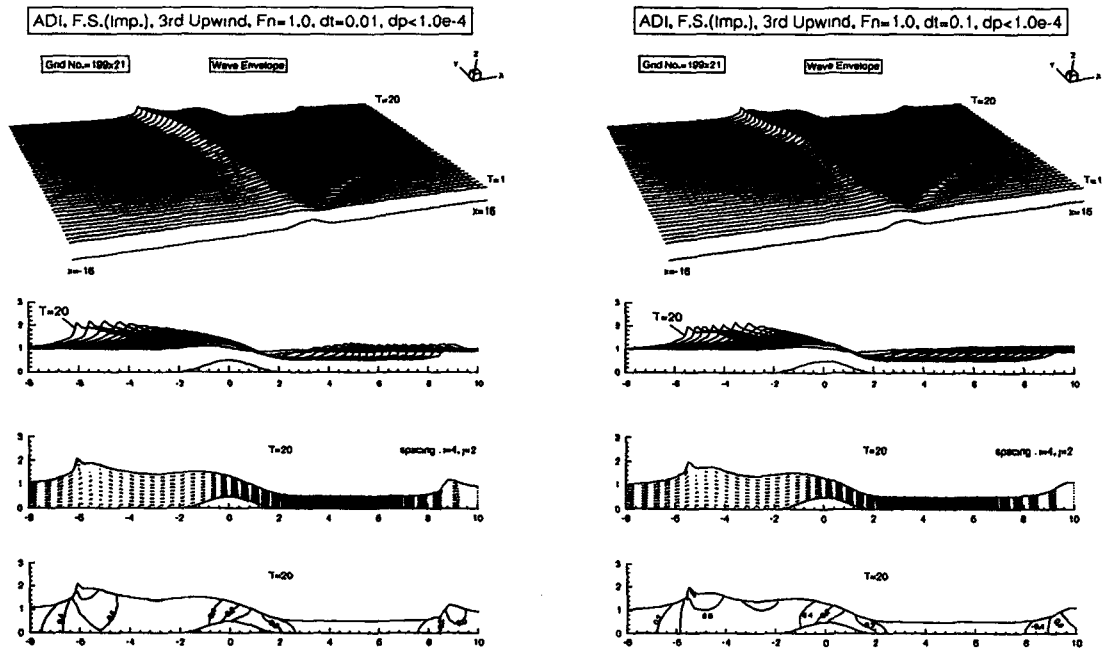

Fig. 2 Comparison of wave profile (ADI : $\Delta t = 0.01,\ 0.1$)

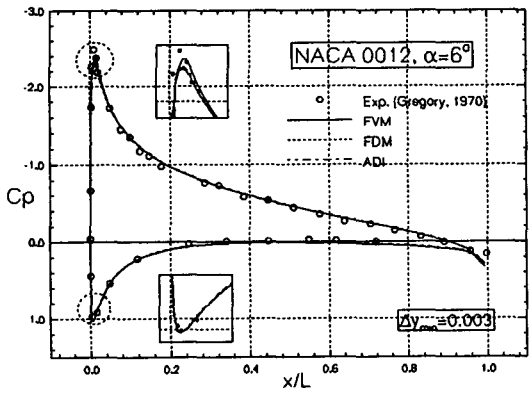

Fig. 3 Comparison of pressure distribution

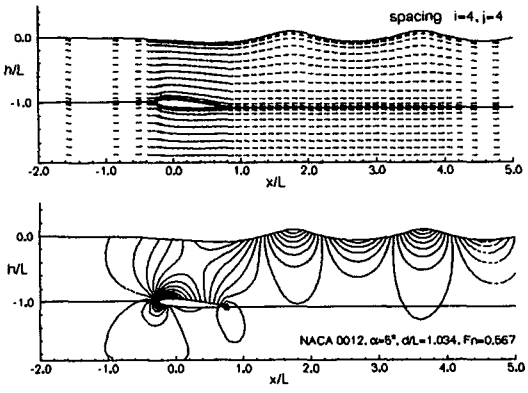

Fig. 4 Velocity vectors and pressure contours

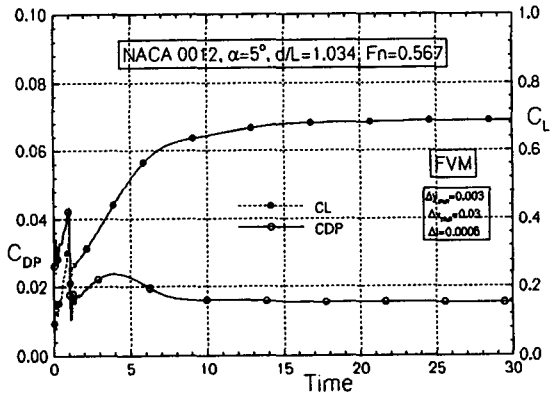

Fig. 5 Convergence history of C_{DF} and C_L

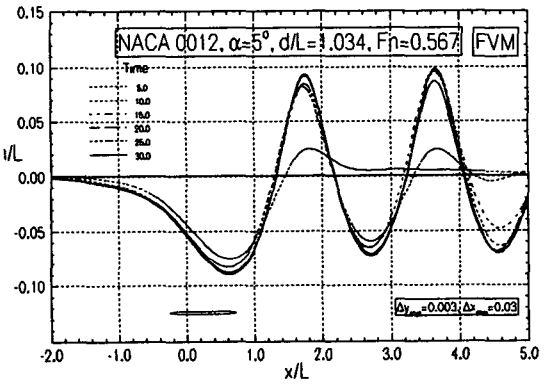

Fig. 6 Convergence history of wave

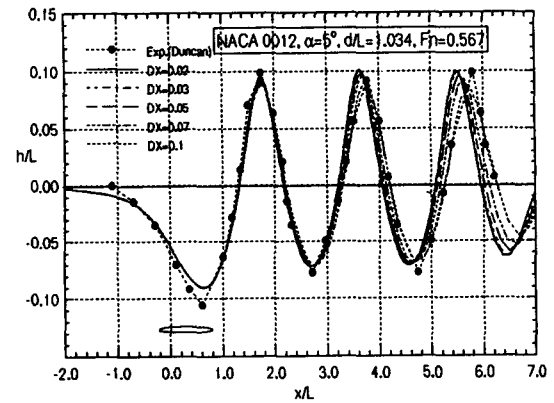

Fig. 7 Wave profiles for various grid sizes

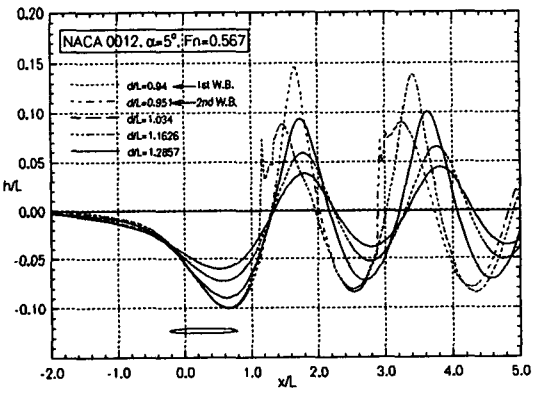

Fig. 8 Wave profiles for various sub. depths